BRCA1 Promotes Induction of ssDNA by Ionizing Radiation

Brian P. Schlegel,[1] Francine M. Jodelka,[1] and Rafael Nunez[2]

[1]Department of Pathology and [2]Section of Hematology/Oncology, University of Illinois Cancer Center, Chicago, Illinois

Abstract

The BRCA1 tumor suppressor contributes to the repair of DNA double-strand breaks (DSB) through homologous recombination, but the mechanism is unknown. The rapid accumulation of BRCA1 into nuclear foci in response to induction of DNA breaks suggests that BRCA1 may function in an early step in the repair pathway. We examined the role of BRCA1 in one such early step, the resection of DSBs to generate ssDNA. The appearance of ssDNA in response to ionizing radiation is similar to that of BRCA1 foci formation, suggesting that the two processes are related. Furthermore, BRCA1 colocalizes to ssDNA sites induced by ionizing radiation. Overexpression of BRCA1 causes an increase in cells exhibiting ssDNA induced by ionizing radiation. Mutant BRCA1 that lacks the COOH-terminal BRCT domain also promotes ssDNA but fails to form nuclear foci. Knockdown of BRCA1 expression reduces ssDNA and Rad51 foci formation in response to ionizing radiation. These results indicate that BRCA1 promotes induction of ssDNA in response to ionizing radiation and accumulates at sites of ssDNA. (Cancer Res 2006; 66(10): 5181-9)

Introduction

Hereditary predisposition to breast and ovarian cancer has been associated with mutations of *BRCA1* (1, 2). The BRCA1 tumor suppressor contributes to the repair of DNA double-strand breaks (DSB) through homologous recombination. Primary cells derived from BRCA1 knockout mice exhibit chromatid breaks and dicentric chromosomes, defects indicative of errors in recombination events (3). BRCA1-deficient mouse embryonic stem cells exhibit lower rates of DSB repair by homologous recombination (4, 5). Several activities have been ascribed directly to BRCA1 using *in vitro* functional assays, including transcriptional activation (6), E3 ubiquitin ligase activity (7, 8), and phosphopeptide-binding activity (9–11). However, the mechanism by which BRCA1 contributes to homologous recombination is unknown.

The repair of DSBs is essential for cell survival, but some repair mechanisms are potentially mutagenic. Nonhomologous end joining involves direct ligation of DNA termini, but processing of DNA ends before ligation can lead to deletions or insertions. Alternatively, repair can proceed through homology-dependent mechanisms. Degradation of one strand at the break produces 3′-overhanging ssDNA (12). The resulting ssDNA can be up to several kilobases in length and can act as a substrate for two types of homology-dependent repair (13). Single-strand annealing can occur when strand resection reveals complimentary strands at both sides of the break site. These regions anneal, and the intervening sequences are removed. Homologous recombination takes place when the ssDNA invades a homologous dsDNA sequence. The complementary sequence acts as a template to extend the damaged strand and replace the lost sequence. Homologous recombination is potentially error-free because the identical sister chromatid sequence can act as the template for repair. In mammalian somatic cells, sequence exchange (crossover) between the damaged chromosome and the sister chromatid template is infrequent (14).

The rapid accumulation of BRCA1 into nuclear foci in response to agents that induce DSBs suggests that BRCA1 functions in an early step in DNA repair (15). Strand resection is an early step common to homology-dependent repair mechanisms. We present evidence that BRCA1 promotes induction of ssDNA in response to ionizing radiation. Furthermore, BRCA1 accumulation at ssDNA sites requires the COOH-terminal domain of BRCA1.

Materials and Methods

Cell culture. MCF10A and HCC1937 cells were obtained from the American Type Culture Collection (ATCC). Cells were maintained according to ATCC guidelines. Cells were exposed to ^{137}Cs using a JL Shepard and Associates model 143-68 irradiator to deliver γ-irradiation at a dose of 10 Gy. The construction of recombinant adenoviruses that express 5′ HA-tagged BRCA1 (amino acids 1-1863) and 5′ HA-tagged BRCA1ΔCT (amino acids 1-1526) has been described previously (16, 17). Adenovirus that expresses LacZ was obtained from Quantum Biotechnologies, Inc. High titer stocks were generated by propagation of virus in 293 cells and purified by CsCl centrifugation according to standard protocols. Virus titer was determined by serial dilution using the Adeno-X Rapid Titer kit (BD Biosciences), which measures infectious particles using an anti-hexon antibody. Cells were infected with the HA-BRCA1 virus at a multiplicity of infection (MOI) of 175 infectious particles/mL and the HA-BRCA1ΔCT or LacZ virus at a MOI of 350 infectious particles/mL. This resulted in equal protein expression 48 hours after infection based on immunoblot analysis.

Short interfering RNA (siRNA) was obtained from commercial sources (Dharmacon and Ambion). siRNA transfection was done using Dharma-FECT (Dharmacon). Cells were transfected using 150 μmol/L siRNA and harvested 24 hours later for immunoblot analysis. BRCA1 A siRNA targets the BRCA1 mRNA sequence AAGGUUUCAAAGCGCCAGUCA as described previously (18), and BRCA1 B siRNA targets the BRCA1 mRNA sequence GCGAGCAAGAGAAUCCCAG. The nonspecific siRNA sense sequence is UAGCGACUAAACACAUCAA and has no perfect match to known human genes.

BRCA1 antibody production. A cDNA sequence encoding amino acids 700-1110 of human BRCA1 was subcloned into pGEX-2TK (Pharmacia). DH5α *Escherichia coli* was transformed with this expression vector, the bacterial lysate was incubated with glutathione-agarose beads (Pharmacia), and the glutathione *S*-transferase (GST)-BRCA1 fusion protein was eluted with 10 μmol/L glutathione. The purified protein was sent to the University of Illinois at Chicago Protein Research Laboratory (Chicago, IL) for antibody antiserum production in rabbits. The IgG fraction was precipitated from the antiserum with a saturated ammonium sulfate solution; the resulting IgG pellet was dissolved in PBS and then dialyzed overnight to remove the ammonium sulfate. The IgG solution was precleared against GST bound to

Note: Supplementary data for this article are available at Cancer Research Online (http://cancerres.aacrjournals.org/).

Requests for reprints: Brian P. Schlegel, Department of Pathology, University of Illinois at Chicago, 3270 Molecular Biology Research Building, 900 South Ashland Avenue, Chicago, IL 60607. Phone: 312-355-0155; Fax: 312-413-7963; E-mail: schlegel@uic.edu.

doi:10.1158/0008-5472.CAN-05-3209

glutathione-agarose beads. The IgG solution was then applied to a CNBr-activated Sepharose column previously bound with purified GST-BRCA1 700-1110 protein and blocked in 1 mol/L ethanolamine (pH 8). The column was washed extensively with PBS, and the BRCA1-specific antibody was eluted at low pH [50 mmol/L glycine (pH 2.3), 150 mmol/L NaCl] and neutralized with one fourth of the elution volume using 0.5 mol/L sodium phosphate buffer (pH 7.7).

Fluorescence microscopy. Cells were grown on glass coverslips coated with poly-L-lysine. For ssDNA detection, MCF10A cells were cultured for 24 hours in the presence of bromodeoxyuridine (BrdUrd; 10 μg/mL; Invitrogen); HCC1937 cells were cultured 48 hours in the presence of BrdUrd due to a longer doubling time. To visualize mitochondria, cells were then incubated for an additional 1 hour in the presence of CytoTracker CMXRos (50 nmol/L; Invitrogen), a cell-permeable fluorescent dye specific for mitochondria. Cells were washed twice with PBS, fixed in methanol for 20 minutes at −20°C, and then briefly dipped in acetone at −20°C. A control sample was included in each experiment to determine the percentage of cells that incorporated BrdUrd. This was done after fixation by incubating the cells in 2 N HCl containing 0.2 mg/mL pepsin for 20 minutes. Alternatively, samples were incubated in 70% formamide with 2× SSC at 80°C for 1 minute and then dehydrated in an alcohol series. After fixation, cells were rehydrated in PBS for 5 minutes and incubated in blocking buffer (PBS, 0.02% NaN_3, 0.2% Triton X-100, 0.05% Tween 20, 0.1% bovine serum albumin, 10% goat serum) for 30 minutes at room temperature. Samples were incubated with the RA81647 anti-BRCA1 rabbit polyclonal antibody (2.6 μg/mL) or an anti-Rad51 rabbit monoclonal antibody (mAb; Ab-1, Calbiochem) and anti-BrdUrd mouse mAb clone B44 (2.5 μg/mL; BD Biosciences) or the anti-BRCA1 mouse mAb Ab-1 (clone MS110, 1 μg/mL; Calbiochem) in blocking buffer overnight at 4°C. The coverslips were washed thrice in PBS for 5 minutes. The samples were incubated with an Alexa Fluor 488–conjugated goat anti-mouse antibody (8 μg/mL) and an Alexa Fluor 555–conjugated goat anti-rabbit antibody (8 μg/mL; Invitrogen) in blocking buffer for 1 hour at room temperature. Samples were mounted on glass slides with mounting medium containing 4′,6-diamidino-2-phenylindole (DAPI; Vectashield).

Samples were viewed at ×1,000 magnification using a Labophot-2 upright fluorescence microscope. Cells were scored positive when ≥10 nuclear foci were visible by focusing through the cell. ssDNA-positive cells were normalized for BrdUrd incorporation. Images were acquired using a Carl Zeiss LSM 510 Meta Laser scanning confocal microscope equipped with a 63× water immersion objective. Beams of 488 nm from Ar laser, 543 nm from HeNe1 laser, and 405 nm from Diode were used for excitation. Green, red, and blue fluorescence emissions were detected through LP 505, 560, and 420 filters, respectively. The three different fluorochromes were scanned sequentially by using multitracking function to avoid any bleed through among those fluorescent dyes. Some images were scanned with zoom 2, resulting in a final ×1,260 magnification.

Immunoblot analysis. Cells were lysed directly on culture plates in 5% SDS containing 10 mmol/L sodium phosphate buffer (pH 7). The lysate was sonicated and then heated in a boiling water bath for 5 minutes. Samples were normalized for total protein, resolved on a 3% to 8% Tris-acetate SDS-PAGE, transferred to a polyvinylidene difluoride membrane, probed with specific antibody, and visualized by chemiluminescence.

Flow cytometry. Cells remaining on the culture plate after the coverslip was removed for immunofluorescence microscopy were trypsinized and fixed overnight in 70% ethanol at −20°C. Cells were resuspended in PBS containing 50 μg/mL propidium iodide (Sigma) and 100 μg/mL RNase A (Fermentas) and incubated for 2 hours at 4°C with rotation. Cell cycle profiles were determined by two-variable flow cytometry using a Becton Dickinson FACSCalibur flow cytometer and CellQuest software (Becton Dickinson). Acquired events were gated to eliminate cell aggregates and debris. A gated population of 2×10^4 single diploid cells was analyzed.

Results

Visualization of ssDNA. To examine if BRCA1 contributes to the strand resection step, we used an assay that permits identification of sites of ssDNA >1 kb *in situ* (13). This assay is based on the observation that the BrdUrd nucleotide base analogue is recognized by an anti-BrdUrd antibody when incorporated into ssDNA but not dsDNA. The assay is similar in principle to the flow cytometric assays used to measure cells in S phase, except that the denaturant is omitted. This approach successfully showed that induction of DSBs promotes ssDNA formation followed by accumulation of replication protein A (RPA) and Rad51 at ssDNA sites (13). We applied this approach to study the appearance of ssDNA in MCF10A cells in response to ionizing radiation. MCF10A cells were chosen because they are an immortalized nontransformed human breast epithelial cell line that expresses wild-type BRCA1. BrdUrd incorporation was visualized by indirect immunofluorescence. In the absence of a denaturing agent, no nuclear staining of BrdUrd is apparent (Fig. 1*A*). After treatment of fixed cells with HCl to denature DNA, BrdUrd labeling appeared uniform throughout the nucleus, whereas staining with DAPI appeared reduced. The vast majority of cells was labeled by 24 hours (Fig. 1*B*). A similar result was obtained when samples were denatured in formamide (data not shown), indicating that nuclear staining is specific for ssDNA.

We also observed extensive cytoplasmic staining that varied somewhat from cell to cell, suggestive of mitochondria. Replication of mitochondrial DNA (mtDNA) is not synchronized with nuclear DNA replication. Furthermore, mitochondria exhibit long stretches of ssDNA (19). Therefore, we might expect to see a cytoplasmic BrdUrd signal even in the absence of a denaturant. To confirm that the cytoplasmic BrdUrd signal represents mtDNA, we stained BrdUrd-labeled cells with a mitochondria-specific stain, MitoTracker Red CMXRos (Supplementary Fig. S1). This cell-permeable fluorescent dye is sequestered by live cells in metabolically active mitochondria and retained on fixation. Dual staining of BrdUrd and mitochondria in unirradiated cells resulted in extensive colocalization of cytoplasmic ssDNA and mitochondria. Virtually all of the ssDNA colocalizes with mitochondria. A few mitochondria do not exhibit ssDNA probably because they have not yet replicated their DNA. We conclude that the cytoplasmic BrdUrd signal reflects mitochondrial ssDNA and is not relevant to interpretation of the nuclear BrdUrd signal induced on exposure to ionizing radiation.

Next, we exposed cells labeled with BrdUrd to ionizing radiation (10 Gy) and incubated for an additional 8 hours. Cells were then fixed without a denaturization step and stained for BrdUrd. Similar to previous reports, we observed staining of BrdUrd as discrete nuclear foci only in a subset of irradiated samples (Fig. 1*C*; refs. 13, 20, 21). Furthermore, when cells were stained concurrently for Rad51, partial colocalization of the two signals was observed (Fig. 1*C*). This supports the possibility that at least some of the ssDNA observed in response to ionizing radiation represents an intermediate in homology-directed DNA repair.

Partial colocalization of BRCA1 and ssDNA in response to ionizing radiation. To stain cells concurrently for ssDNA and BRCA1, it is necessary to use a polyclonal antibody directed against BRCA1. We generated a rabbit polyclonal antibody directed against amino acid residues 700-1110 of BRCA1. The affinity-purified antibody recognizes *in vitro*–translated BRCA1 (Supplementary Fig. S2A). It produced an identical nuclear staining pattern in irradiated cells as mouse MS110 mAb, one of the first and best characterized antibodies directed against BRCA1 (Supplementary Fig. S2B; ref. 22). We again exposed cells labeled with BrdUrd to ionizing radiation (10 Gy), incubated for 8 hours, and stained for ssDNA and

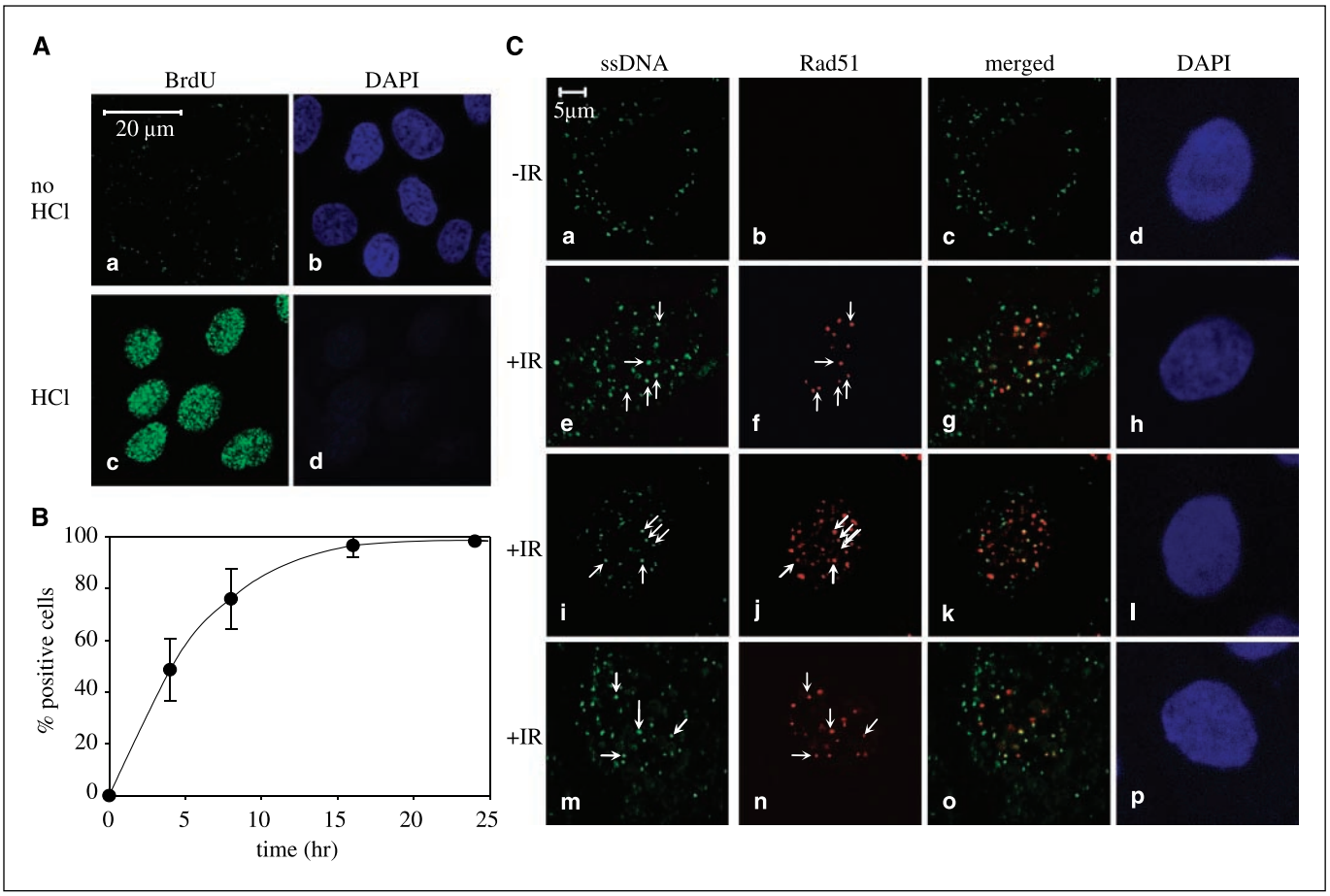

Figure 1. Detection of ssDNA in response to ionizing radiation. *A,* BrdUrd incorporation into DNA provides a marker for ssDNA. MCF10A cells were grown in the presence of BrdUrd (10 μg/mL) for 24 hours and then fixed and stained with a mouse monoclonal anti-BrdUrd antibody followed by an Alexa Fluor 488–conjugated anti-mouse antibody to visualize ssDNA. Untreated cells do not stain positive for BrdUrd (*a*), whereas cells treated with 2 N HCl after fixation to denature DNA are strongly positive (*c*). *b* and *d,* DAPI counterstain is specific for dsDNA. *B,* time course for BrdUrd incorporation into DNA. *Points,* mean of three or more independent experiments; *bars,* SD. A minimum of 100 cells was scored for each experiment. *C,* partial colocalization of ssDNA and Rad51 in response to ionizing radiation (*IR*). MCF10A cells were grown as in (*A*), treated with γ-irradiation (10 Gy), and incubated for an additional 8 hours. The cells were then fixed and stained for ssDNA and Rad51 using a polyclonal antibody specific for Rad51 and an Alexa Fluor 555–conjugated anti-rabbit antibody to visualize Rad51. ssDNA (*a, e, i*, and *m; green*) and Rad51 nuclear foci (*b, f, j*, and *n; red*) were only visible in response to ionizing radiation (*e-p*). *c, g, k,* and *o,* colocalization of ssDNA and Rad51. *Arrows,* specific foci.

BRCA1 using our affinity-purified polyclonal antibody. We observed a subset of cells that exhibited ssDNA and BRCA1 nuclear foci. These cells also exhibited partial colocalization of ssDNA and BRCA1 (Fig. 2*A*), consistent with the putative role of BRCA1 in homology-directed repair.

Kinetics of ssDNA and BRCA1 foci formation in response to ionizing radiation. Next, we examined if ssDNA and BRCA1 foci form over a similar time course in response to ionizing radiation. To quantitate nuclear foci, we examined cells at ×1,000 magnification, making it easy to distinguish nuclear foci from the cytoplasmic background. Cells were scored as positive when ≥10 foci were observed while focusing through the nucleus. A minimum of 100 cells was scored for each of three or more independent experiments. We first observed ssDNA in a subset of cells as discrete nuclear foci 1 hour after irradiation (Fig. 2*B*). The number of cells positive for ssDNA sites peaked at ~40% between 4 and 8 hours after irradiation. Only ~10% of the cells were positive for ssDNA 24 hours after irradiation.

Although a comparable trend was apparent for BRCA1-positive cells, there are some distinct differences. About 5% of cells exhibit BRCA1 nuclear foci even without treatment with ionizing radiation. After irradiation, BRCA1 nuclear foci appeared within 20 minutes. These foci were less intense than BRCA1 foci apparent before irradiation. Similar to ssDNA-positive cells, the number of cells positive for BRCA1 foci peaked between 4 and 8 hours after irradiation, and only ~10% of the cells were positive for BRCA1 24 hours after irradiation (Fig. 2*B*). The similar appearance of the kinetic profiles of ssDNA and BRCA1 foci formation suggests that the two processes are related. We observed that virtually all cells that were positive for ssDNA also exhibited some BRCA1 focus formation. However, ~20% of cells positive for BRCA1 foci between 4 and 8 hours after irradiation did not exhibit ssDNA foci (Fig. 2*B*). In addition, BRCA1 foci became more intense over the same time course (Fig. 2*C*). Confocal microscope settings were optimized for the faint BRCA1 foci at the earliest time point, and images were acquired without changing settings between samples. Therefore, the progressively larger foci represent an increase in signal intensity. This suggests that BRCA1 may accumulate at sites of ssDNA over time.

Overexpression of BRCA1 promotes ssDNA formation in response to ionizing radiation. The partial colocalization of ssDNA and BRCA1 and the similar kinetic profiles of foci formation

suggest an early role for BRCA1 in DNA repair. However, the observation that BRCA1 associates with Rad51 suggests that BRCA1 functions at a late step in homology-dependent repair (23). We examined ssDNA formation in response to ionizing radiation in HCC1937 cells. HCC1937 is a human breast epithelial tumor cell line that is homozygous for the *BRCA1* 5382insC mutation. The resulting protein product lacks a functional BRCT domain that is required for tumor suppressor activity (24). Hypersensitivity of these cells to ionizing radiation is abrogated by expression of full-length BRCA1 (25). However, these cells exhibit Rad51 formation in response to ionizing radiation (26), suggesting that resection of DSBs still occurs. We infected HCC1937 cells with a recombinant adenovirus that expresses full-length HA-tagged BRCA1 or a COOH-terminal deletion mutant (Fig. 3*A*). Infected cells were labeled with BrdUrd, exposed to ionizing radiation (10 Gy), fixed at various times, stained for ssDNA, and scored as described previously (Fig. 3*B*). Surprisingly, ~5% of uninfected HCC1937 cells exhibited ssDNA sites even without exposure to ionizing radiation. Treatment of cells with ionizing radiation further increased the number of ssDNA-positive cells (Fig. 3*B*). Unlike MCF10A cells, the percentage of cells positive for ssDNA did not decrease by 24 hours, consistent with the observed hypersensitivity to ionizing radiation. Overexpression of full-length BRCA1 did not alter the early kinetics of ssDNA formation, but by 24 hours, there was a 2-fold increase in the percentage of ssDNA-positive cells in response to ionizing radiation (Fig. 3*B*). This observation is consistent with a role for BRCA1 in strand resection in response to DSBs. Overexpression of the truncated form of BRCA1 that lacks

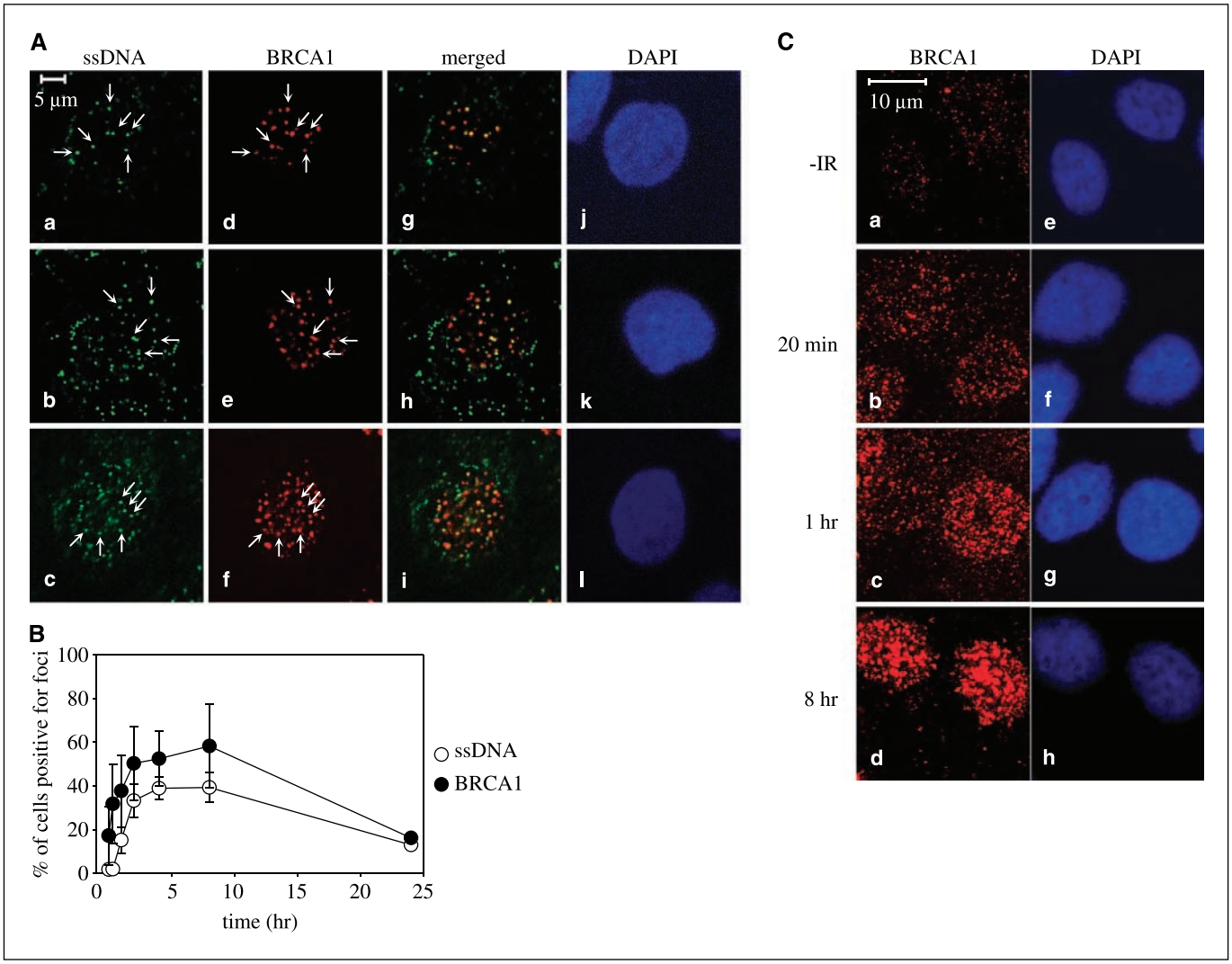

Figure 2. Induction of ssDNA and BRCA1 foci by ionizing radiation. *A,* partial colocalization of BRCA1 and ssDNA in response to ionizing radiation. MCF10A cells were grown in the presence of BrdUrd (10 μg/mL) for 24 hours, treated with γ-irradiation (10 Gy), and incubated for an additional 8 hours. The cells were then fixed and stained for ssDNA and BRCA1 using mouse monoclonal anti-BrdUrd antibody and a polyclonal antibody specific for BRCA1 followed by an Alexa Fluor 488–conjugated anti-mouse antibody and an Alexa Fluor 555–conjugated anti-rabbit antibody to visualize ssDNA and BRCA1, respectively. ssDNA (*a-c; green*) and BRCA1 nuclear foci (*d-f; red*) were only visible in response to ionizing radiation. *g* to *i,* colocalization of ssDNA and BRCA1. *j* to *l,* DAPI counterstain is specific for dsDNA. *Arrows,* specific foci. *B,* kinetics of ionizing radiation induced ssDNA and BRCA1 foci formation. The appearance of ssDNA and BRCA1 foci follow a similar time course in response to ionizing radiation. MCF10A cells were treated as in (*A*) but fixed after irradiation at the indicated times. Cells exhibiting ≥10 foci per nuclei were scored as positive. A minimum of 100 cells was scored for each experiment. *Points,* mean of three or more independent experiments; *bars,* SD. *C,* progressive accumulation of BRCA1 in foci in response to ionizing radiation. MCF10A cells were treated as in (*B*) but without visualization of ssDNA. Scanning settings were held constant for each separate sample so that BRCA1 intensities could be compared directly.

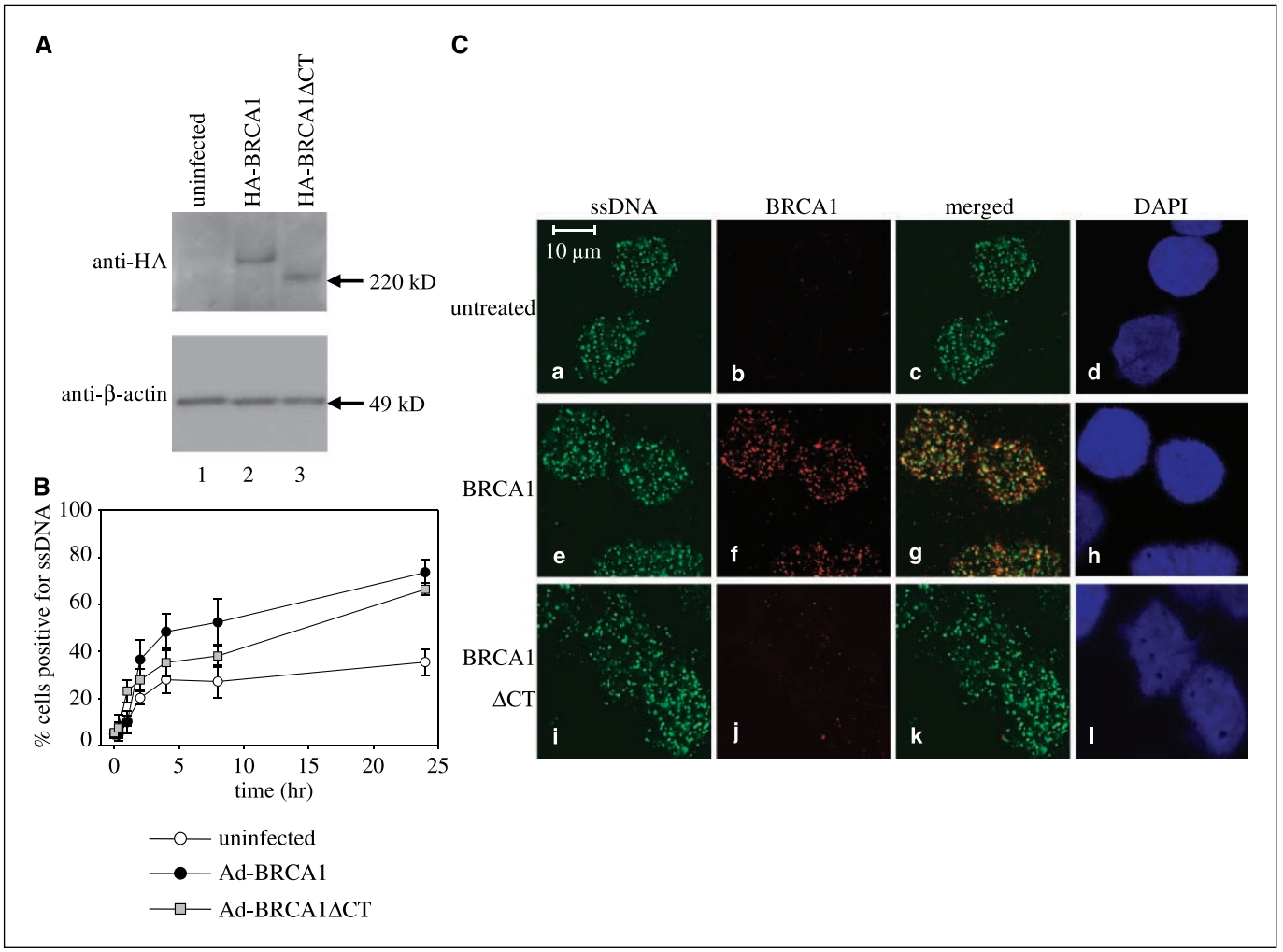

Figure 3. Overexpression of BRCA1 in HCC1937 cells promotes ssDNA formation in response to ionizing radiation. *A,* immunoblot analysis of HCC1937 cells infected with a recombinant adenovirus that expresses full-length HA-BRCA1 (amino acids 1-1863) or a truncated form of BRCA1 that lacks the COOH-terminal domain (HA-BRCA1ΔCT; amino acids 1-1527). Lysate protein was resolved by SDS-PAGE and visualized using an anti-HA or anti-β-actin antibody. *B,* overexpression of full-length and truncated BRCA1 promotes ssDNA formation in response to ionizing radiation. HCC1937 cells were infected with recombinant adenovirus (*Ad*) and grown in the presence of BrdUrd (10 μg/mL) for 48 hours. Cells were then treated with γ-irradiation (10 Gy), fixed at the indicated times, and stained for ssDNA. *C,* the COOH-terminal domain of BRCA1 is required for accumulation at sites of ssDNA. Uninfected HCC1937 cells (*a-d*) and cells infected with recombinant adenovirus that expresses full-length BRCA1 (*e-h*) or truncated BRCA1ΔCT (*i-l*) were treated as in (*B*), except that cells were also stained with a polyclonal antibody specific for BRCA1.

the COOH-terminal BRCT domain also caused an increase in ssDNA-positive cells in response to ionizing radiation by 24 hours. This is not simply a result of adenovirus infection because infection of HCC1937 cells with a recombinant adenovirus alone does not result in an increase in ssDNA-positive cells in response to ionizing radiation. Overexpression of full-length or mutant BRCA1 does not alter the cell cycle profile of HCC1937 cells, indicating that the increase in ssDNA-positive cells 24 hours after irradiation is not a function of cell cycle progression (Supplementary Fig. S3). We conclude that the COOH-terminal domain of BRCA1 is not required for formation of ssDNA in response to ionizing radiation.

Endogenous truncated BRCA1 did not colocalize with sites of ssDNA on irradiation (Fig. 3*C*). The overexpressed full-length protein formed foci and colocalized with sites of ssDNA, whereas the exogenous truncation mutant did not (Fig. 3*C*). This observation is consistent with the previous finding that the BRCA1 COOH terminal is required for foci formation in response to ionizing radiation (27). We conclude that although the BRCA1 COOH-terminal deletion mutant cannot form nuclear foci in response to ionizing radiation, it may still promote ssDNA formation.

Knockdown of BRCA1 expression reduces ssDNA formation in response to ionizing radiation. To confirm the role of BRCA1 in ssDNA formation in response to ionizing radiation, we knocked down expression of BRCA1 in MCF10A cells by RNA interference (RNAi) and measured ssDNA foci formation in response to ionizing radiation. Exponentially growing cells were transfected with one of two BRCA1-specific siRNAs and labeled with BrdUrd. Immunoblot analysis of cell lysate indicates a substantial reduction in BRCA1 protein levels 24 hours after transfection of BRCA1-specific siRNAs compared with mock-transfected cells or cells transfected with a nonspecific siRNA (Fig. 4*A*). Cells were irradiated 24 hours after transfection and incubated for an additional 8 hours to allow BRCA1 foci to form. Immunofluorescence staining of irradiated cells indicated a substantial reduction

in BRCA1 protein levels 24 hours after transfection (Fig. 4*B*). The number of cells positive for BRCA1 foci was significantly reduced in cells transfected with BRCA1-specific siRNAs, whereas there was no significant change in the control samples (Fig. 5*A*). A similar effect was observed on ssDNA focus formation in response to ionizing radiation (Fig. 5*B*). Indeed, entire fields of cells did not exhibit either ssDNA or BRCA1 focus formation in response to ionizing radiation (Fig. 4*C*). Normally, we observed ssDNA and BRCA1-positive cells distributed throughout irradiated control samples.

One explanation for the decrease in ssDNA-positive cells is that the decrease in BRCA1 expression alters the cell cycle profile in response to ionizing radiation. Cells that lack functional BRCA1 do not exhibit a mitotic checkpoint (28). Therefore, accumulation of cells in G_1 after exposure to ionizing radiation may prevent strand resection because the nonhomologous end-joining pathway predominates during that phase of the cell cycle. Flow cytometric analysis indicated that knockdown of BRCA1 expression did not affect the cell cycle profile of irradiated cells (Supplementary Fig. S4). The decrease in ssDNA-positive cells cannot be attributed to changes in cell cycle progression in response to loss of BRCA1.

Consistent with the observed decrease in ssDNA formation, knockdown of BRCA1 also resulted in a decrease in Rad51 foci formation in response to ionizing radiation. MCF10A cells were transfected with one of two BRCA1-specific siRNAs and labeled with BrdUrd. Immunofluorescence staining of irradiated cells indicates a substantial reduction in Rad51 foci formation 24 hours after transfection of BRCA1-specific siRNAs compared with mock-transfected cells or cells transfected with a nonspecific siRNA (Fig. 6*A*). Cells were irradiated 24 hours after transfection and incubated for an additional 8 hours to allow Rad51 foci to form. The number of cells positive for Rad51 foci was significantly reduced in cells transfected with BRCA1-specific siRNAs, whereas

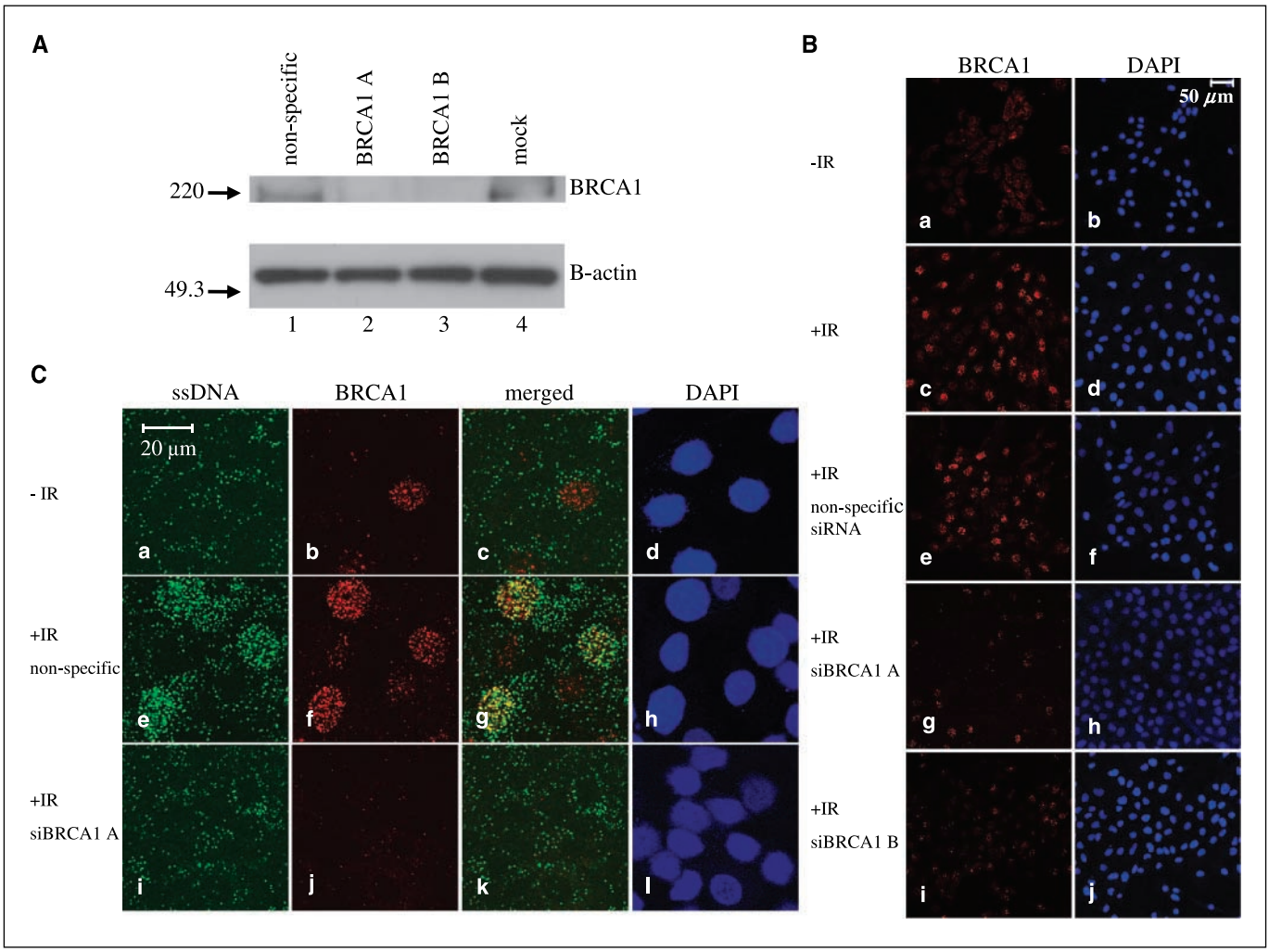

Figure 4. Knockdown of BRCA1 expression by siRNA. *A,* immunoblot analysis of lysate from MCF10A cells transfected with siRNA specific for BRCA1. Cells were mock transfected (*lane 4*), transfected with a nonspecific siRNA (*lane 1*), or transfected with one of two siRNAs specific for BRCA1 (*lanes 2* and *3*). Cells were harvested 24 hours after transfection. Lysate protein was resolved by SDS-PAGE and visualized using an anti-BRCA1 or anti-β-actin antibody. *B,* immunofluorescence analysis of cells transfected with BRCA1-specific siRNAs. Cells were transfected as in (*A*), treated with γ-irradiation (10 Gy) 24 hours later (except *−IR*), incubated for an additional 8 hours, and then fixed and stained for BRCA1. *C,* ssDNA foci formation is reduced in response to ionizing radiation after knockdown of BRCA1 expression. Samples were treated as in (*B*), except cells were also incubated in the presence of BrdUrd (10 μg/mL) immediately after transfection and stained to visualize BRCA1 and ssDNA foci after irradiation. High magnification is used to illustrate the decrease in ssDNA because nuclear ssDNA is difficult to visualize clearly under low magnification. Magnification, ×250 versus ×1,280.

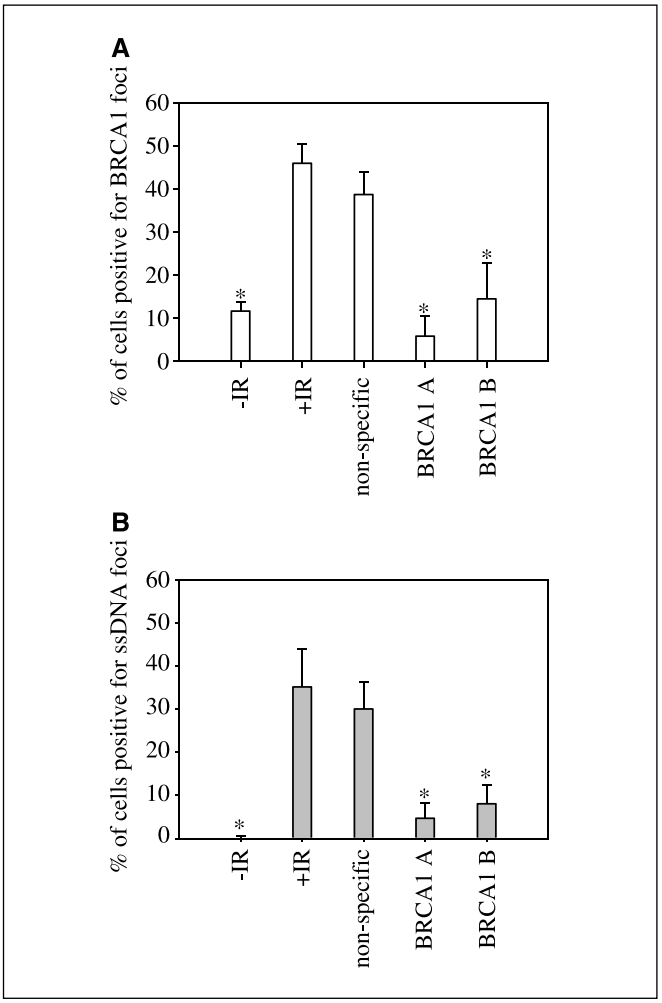

Figure 5. Knockdown of BRCA1 expression reduces ssDNA formation in response to ionizing radiation. *A,* knockdown of BRCA1 levels in MCF10A cells. Cells were mock transfected (*−IR* and *+IR*) or transfected with a nonspecific siRNA or one of two BRCA1-specific siRNAs (*BRCA1 A* and *BRCA1 B*). Cells were treated with γ-irradiation (10 Gy) 24 hours later (except *−IR*), incubated for an additional 8 hours, and then fixed and stained for BRCA1. *, $P \leq 0.01$, compared with irradiated control (*+IR*). *Bars,* SD. *B,* same as (*A*), except cells were grown in the presence of BrdUrd (10 μg/mL) immediately after transfection and stained for ssDNA after irradiation.

there was no significant change in the control samples (Fig. 6*B*). A similar effect was observed on ssDNA focus formation in response to ionizing radiation (Fig. 6*C*). Immunoblot analysis of cell lysate from transfected cells did not show a change in Rad51 expression (Fig. 6*D*), indicating that the decrease in Rad51 foci formation is not a result of decrease protein expression.

Discussion

Several lines of evidence support the conclusion that BRCA1 promotes formation of ssDNA in response to ionizing radiation. First, the appearance of BRCA1 foci exhibits a similar time course as ssDNA, suggesting that BRCA1 is involved in the formation and resolution of the ssDNA intermediate during DSB repair. Consistent with this observation, BRCA1 inhibits the 3′ to 5′ exonuclease activity of the Mre11-Rad50-Nbs1 complex *in vitro*, indicating that BRCA1 binds to the ends of DSBs (29). Second, a fraction of ssDNA foci colocalizes with BRCA1 as early as 1 hour after irradiation. Third, overexpression of BRCA1 increases the percentage of cells that form ssDNA in response to ionizing radiation. This is possibly due to artificially high levels of BRCA1 in cells during G_1. The increase in BRCA1 may promote strand resection in a population of cells where nonhomologous end joining normally predominates. Fourth, knockdown of BRCA1 expression causes a decrease in cells that form ssDNA in response to ionizing radiation, indicating that BRCA1 promotes ssDNA foci formation in response to induction of DSBs. Analysis of homology-dependent repair frequencies in BRCA1-deficient cells supports a role for BRCA1 in strand resection. Repair of DSBs through both homologous recombination and single-strand annealing is reduced in BRCA1-deficient mouse embryonic stem cells (30). Strand resection is a step common to both pathways. However, our data do not rule out an indirect mechanism for promotion of strand resection, such as transcriptional regulation.

It is not certain that ssDNA, measured using the BrdUrd incorporation assay, represents an intermediate in homology-directed DNA repair. However, the ssDNA is observed in response to DNA-damaging agents that induce DSBs, such as ionizing radiation. Furthermore, several proteins involved in homologous recombination, such as Rad51, BLM, PLM, and TopBP1, have been shown to colocalize with ssDNA in response to ionizing radiation when visualized by this method (13, 20, 21). We have also shown that knockdown of BRCA1 expression reduces both ssDNA formation and Rad51 focus formation in response to ionizing radiation. Therefore, ssDNA, visualized using BrdUrd incorporation, likely reflects resection of DSBs.

Colocalization of BRCA1 with ssDNA requires the BRCT domain, whereas ssDNA formation does not, indicating that the two activities may be distinguishable. BRCA1-deficient mouse embryonic stem cells exhibit reduced Rad51 foci in response to ionizing radiation (31), possibly because strand resection is not as efficient in the absence of functional BRCA1. HCC1937 cells form RPA and Rad51 foci in response to ionizing radiation (26, 32) because the truncated form of BRCA1 present in these cells can still promote ssDNA formation.

A single report claims that BRCA1 is not required for Rad51 focus formation in human breast and ovarian tumor cells in response to ionizing radiation (33). Assuming that Rad51 foci represent ssDNA sites, this observation is not consistent with the data obtained using the BRCA1-deficient mouse embryonic stem cells or with our current findings. The inconsistency is likely due to the amount of functional BRCA1 present in the cells used in each study. Retroviral-mediated knockdown of BRCA1 by RNAi, the technique used in the aforementioned study, is not likely to decrease BRCA1 expression as completely as direct transfection of siRNA. We observe that BRCA1 focus formation is not necessary for strand resection. Hundreds or thousands of BRCA1 molecules must be present to be visible as foci, but as little as one BRCA1 molecule per DSB may be sufficient for ssDNA formation. Therefore, a modest decrease in BRCA1 expression may affect BRCA1 focus formation but not ssDNA or Rad51 focus formation.

We conclude that BRCA1 promotes ssDNA formation in response to ionizing radiation and then accumulates at ssDNA sites. A large number of functions have been attributed to BRCA1, such as roles in transcription (6, 34–37), ubiquitination (7, 8, 38, 39), signaling of DNA damage (40–42), and checkpoint control (28, 43–45). However, it is unknown which, if any, of these functions contribute to the strand resection function. We propose

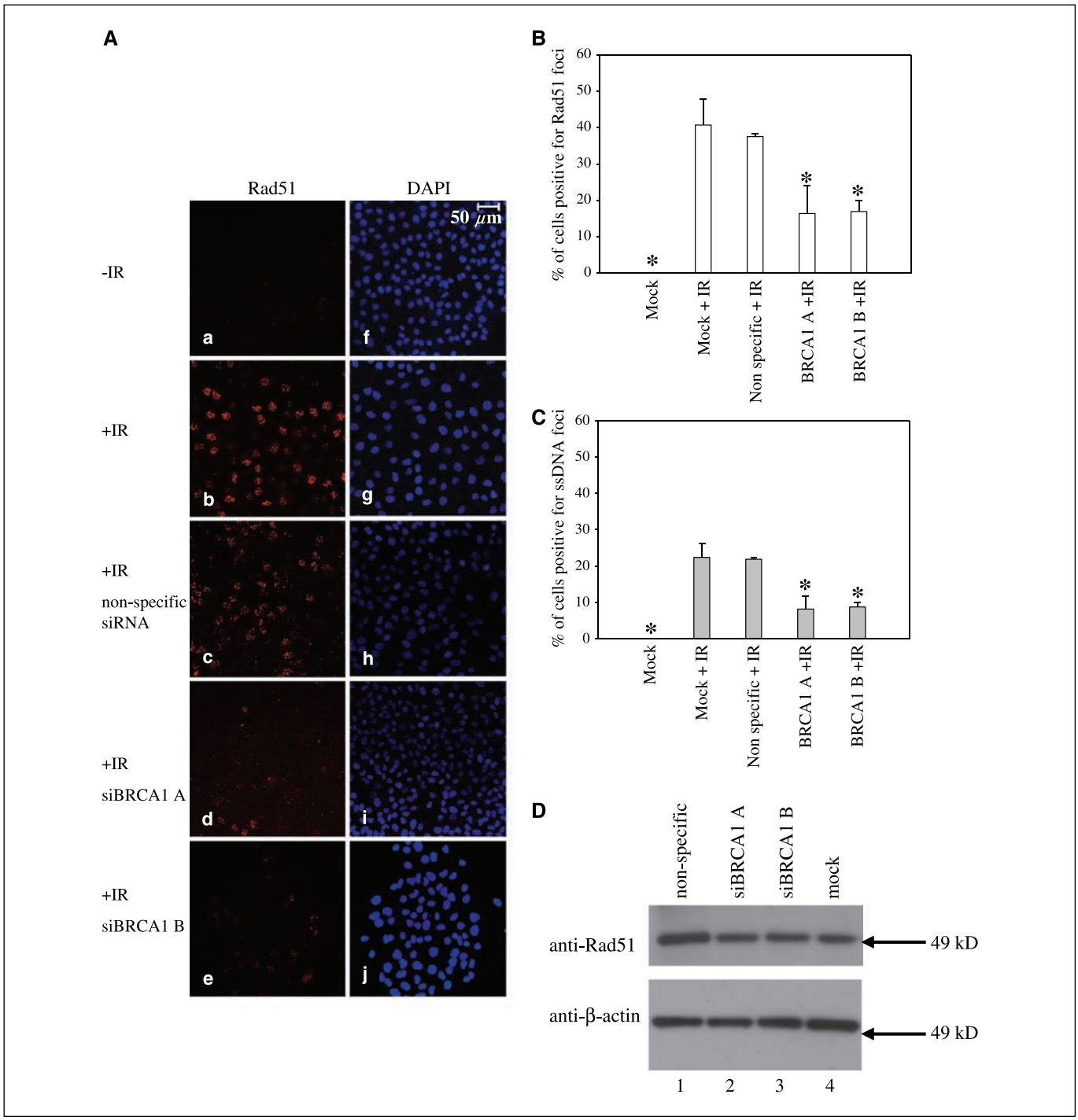

Figure 6. Knockdown of BRCA1 expression reduces Rad51 foci formation in response to ionizing radiation. *A,* decrease in Rad51 foci formation in response to ionizing radiation in cells transfected with BRCA1-specific siRNA. Cells were mock transfected (*−IR* and *+IR*) or transfected with a nonspecific siRNA or one of two BRCA1 specific siRNAs (*BRCA1 A* and *BRCA1 B*). Cells were treated with γ-irradiation (10 Gy) 24 hours later (except *−IR*), incubated for an additional 8 hours, and then fixed and stained for Rad51 (*a-e*) and counterstained with DAPI to visualize the nuclei (*f-j*). *B,* quantification of Rad51 foci formation. MCF10A cells were treated as in (*A*) and scored for Rad51 foci formation. Cells exhibiting ≥10 foci per nuclei were scored as positive. A minimum of 100 cells was scored for each experiment. *Columns,* mean of three or more independent experiments; *bars,* SD. *, $P \leq 0.01$, compared with irradiated control (*+IR*). *C,* quantification of ssDNA formation. Same as (*B*), except cells were grown in the presence of BrdUrd (10 μg/mL) immediately after transfection and then fixed, stained, and scored for ssDNA after irradiation. *D,* knockdown of BRCA1 expression does not reduce Rad51 expression. Immunoblot analysis of Rad51 expression in cells transfected with BRCA1-specific siRNA as described in (*A*) but without irradiation. Lysate protein was resolved by SDS-PAGE and visualized using an anti-Rad51 or an anti-β-actin antibody.

a model where BRCA1 functions directly in resection of DSBs. BRCA1 is required for the exonuclease and/or helicase activities at DSBs that contribute to strand resection. This may be a result of direct recruitment of factors by BRCA1 to break sites or through indirect mechanisms, such as chromatin modification or transcriptional regulation. BRCA1 then accumulates at the resulting ssDNA sites, possibly contributing to a later step in homology-dependent repair.

Acknowledgments

Received 9/6/2005; revised 3/6/2006; accepted 3/17/2006.

Grant support: Illinois Division of the American Cancer Society grant 04-01, American Cancer Society Institutional Research grant 99-224, and University of Illinois Campus Research Board grant (B.P. Schlegel).

The costs of publication of this article were defrayed in part by the payment of page charges. This article must therefore be hereby marked *advertisement* in accordance with 18 U.S.C. Section 1734 solely to indicate this fact.

We thank M. Chen and the Research Resource Center (University of Illinois at Chicago) for assistance with confocal microscopy and B. Lee and the Protein Research Laboratory (University of Illinois at Chicago) for antibody production.

References

1. Miki Y, Swensen J, Shattuck-Eidens D, et al. Strong candidate for the breast and ovarian cancer susceptibility gene BRCA1. Science 1994;266:66–71.
2. Ford D, Easton DF, Stratton M, et al. Genetic heterogeneity and penetrance analysis of the BRCA1 and BRCA2 genes in breast cancer families. The Breast Cancer Linkage Consortium. Am J Hum Genet 1998;62:676–89.
3. Shen SX, Weaver Z, Xu X, et al. A targeted disruption of the murine Brca1 gene causes γ-irradiation hypersensitivity and genetic instability. Oncogene 1998;17:3115–24.
4. Snouwaert JN, Gowen LC, Latour AM, et al. BRCA1 deficient embryonic stem cells display a decreased homologous recombination frequency and an increased frequency of non-homologous recombination that is corrected by expression of a Brca1 transgene. Oncogene 1999;18:7900–7.
5. Moynahan ME, Chiu JW, Koller BH, Jasin M. Brca1 controls homology-directed DNA repair. Mol Cell 1999;4:511–8.
6. Haile DT, Parvin JD. Activation of transcription *in vitro* by the BRCA1 carboxyl-terminal domain. J Biol Chem 1999;274:2113–7.
7. Lorick KL, Jensen JP, Fang S, Ong AM, Hatakeyama S, Weissman AM. RING fingers mediate ubiquitin-conjugating enzyme (E2)-dependent ubiquitination. Proc Natl Acad Sci U S A 1999;96:11364–9.
8. Hashizume R, Fukuda M, Maeda I, et al. The RING heterodimer BRCA1-1 is a ubiquitin ligase inactivated by a breast cancer-derived mutation. J Biol Chem 2001;276:14537–40.
9. Manke IA, Lowery DM, Nguyen A, Yaffe MB. BRCT repeats as phosphopeptide-binding modules involved in protein targeting. Science 2003;302:636–9.
10. Yu X, Chini CC, He M, Mer G, Chen J. The BRCT domain is a phospho-protein binding domain. Science 2003;302:639–42.
11. Rodriguez M, Yu X, Chen J, Songyang Z. Phosphopeptide binding specificities of BRCA1 COOH-terminal (BRCT) domains. J Biol Chem 2003;278:52914–8.
12. Sun H, Treco D, Szostak JW. Extensive 3′-overhanging, single-stranded DNA associated with the meiosis-specific double-strand breaks at the ARG4 recombination initiation site. Cell 1991;64:1155–61.
13. Raderschall E, Golub EI, Haaf T. Nuclear foci of mammalian recombination proteins are located at single-stranded DNA regions formed after DNA damage. Proc Natl Acad Sci U S A 1999;96:1921–6.
14. Johnson RD, Jasin M. Sister chromatid gene conversion is a prominent double-strand break repair pathway in mammalian cells. EMBO J 2000;19:3398–407.
15. Paull TT, Rogakou EP, Yamazaki V, Kirchgessner CU, Gellert M, Bonner WM. A critical role for histone H2AX in recruitment of repair factors to nuclear foci after DNA damage. Curr Biol 2000;10:886–95.
16. Chiba N, Parvin JD. Redistribution of BRCA1 among four different protein complexes following replication blockage. J Biol Chem 2001;276:38549–4.
17. Chiba N, Parvin JD. The BRCA1 and BARD1 association with the RNA polymerase II holoenzyme. Cancer Res 2002;62:4222–8.
18. Starita LM, Machida Y, Sankaran S, et al. BRCA1-dependent ubiquitination of γ-tubulin regulates centrosome number. Mol Cell Biol 2004;24:8457–66.
19. Fernandez-Silva P, Enriquez JA, Montoya J. Replication and transcription of mammalian mitochondrial DNA. Exp Physiol 2003;88:41–56.
20. Bischof O, Kim SH, Irving J, Beresten S, Ellis NA, Campisi J. Regulation and localization of the Bloom syndrome protein in response to DNA damage. J Cell Biol 2001;153:367–80.
21. Xu ZX, Timanova-Atanasova A, Zhao RX, Chang KS. PML colocalizes with and stabilizes the DNA damage response protein TopBP1. Mol Cell Biol 2003;23:4247–56.
22. Scully R, Ganesan S, Brown M, De Caprio JA, Cannistra SA, Feuneun J, et al. Location of BRCA1 in human and breast ovarian cancer cells. Science 1996;272:123–6.
23. Scully R, Chen J, Plug A, et al. Association of BRCA1 with Rad51 in mitotic and meiotic cells. Cell 1997;88:265–75.
24. Tomlinson GE, Chen TT, Stastny VA, et al. Characterization of a breast cancer cell line derived from a germ-line BRCA1 mutation carrier. Cancer Res 1998;58:3237–42.
25. Scully R, Ganesan S, Vlasakova K, Chen J, Socolovsky M, Livingston DM. Genetic analysis of BRCA1 function in a defined tumor cell line. Mol Cell 1999;4:1093–9.
26. Yuan SS, Lee SY, Chen G, Song M, Tomlinson GE, Lee EY. BRCA2 is required for ionizing radiation-induced assembly of Rad51 complex *in vivo*. Cancer Res 1999;59:3547–51.
27. Au WW, Henderson BR. The BRCA1 RING and BRCT domains cooperate in targeting BRCA1 to ionizing radiation-induced foci. J Biol Chem 2005;280:6993–7001.
28. Xu X, Weaver Z, Linke SP, et al. Centrosome amplification and a defective G_2-M cell cycle checkpoint induce genetic instability in BRCA1 exon 11 isoform-deficient cells. Mol Cell 1999;3:389–95.
29. Paull TT, Cortez D, Bowers B, Elledge SJ, Gellert M. Direct DNA binding by Brca1. Proc Natl Acad Sci U S A 2001;98:6086–91.
30. Stark JM, Pierce AJ, Oh J, Pastink A, Jasin M. Genetic steps of mammalian homologous repair with distinct mutagenic consequences. Mol Cell Biol 2004;24:9305–16.
31. Bhattacharyya A, Ear US, Koller BH, Weichselbaum RR, Bishop DK. The breast cancer susceptibility gene BRCA1 is required for subnuclear assembly of Rad51 and survival following treatment with the DNA cross-linking agent cisplatin. J Biol Chem 2000;275:23899–903.
32. Choudhary SK, Li R. BRCA1 modulates ionizing radiation-induced nuclear focus formation by the replication protein A p34 subunit. J Cell Biochem 2002;84:666–74.
33. Zhou C, Huang P, Liu J. The carboxyl-terminal of BRCA1 is required for subnuclear assembly of RAD51 after treatment with cisplatin but not ionizing radiation in human breast and ovarian cancer cells. Biochem Biophys Res Commun 2005;336:952–60.
34. Chapman MS, Verma IM. Transcriptional activation by BRCA1. Nature 1996;382:678–9.
35. Monteiro AN, August A, Hanafusa H. Evidence for a transcriptional activation function of BRCA1 C-terminal region. Proc Natl Acad Sci U S A 1996;93:13595–9.
36. Schlegel BP, Green VJ, Ladias JA, Parvin JD. BRCA1 interaction with RNA polymerase II reveals a role for hRPB2 and hRPB10α in activated transcription. Proc Natl Acad Sci U S A 2000;97:3148–53.
37. Krum SA, Miranda GA, Lin C, Lane TF. BRCA1 associates with processive RNA polymerase II. J Biol Chem 2003;278:52012–20.
38. Mallery DL, Vandenberg CJ, Hiom K. Activation of the E3 ligase function of the BRCA1/BARD1 complex by polyubiquitin chains. EMBO J 2002;21:6755–62.
39. Starita LM, Horwitz AA, Keogh MC, Ishioka C, Parvin JD, Chiba N. BRCA1/BARD1 ubiquitinate phosphorylated RNA polymerase II. J Biol Chem 2005;280:24498–505.
40. Cortez D, Wang Y, Qin J, Elledge SJ. Requirement of ATM-dependent phosphorylation of brca1 in the DNA damage response to double-strand breaks. Science 1999;286:1162–6.
41. Chen J. Ataxia telangiectasia-related protein is involved in the phosphorylation of BRCA1 following deoxyribonucleic acid damage. Cancer Res 2000;60:5037–9.
42. Lee JS, Collins KM, Brown AL, Lee CH, Chung JH. hCds1-mediated phosphorylation of BRCA1 regulates the DNA damage response. Nature 2000;404:201–4.
43. Xu B, Kim S, Kastan MB. Involvement of Brca1 in S-phase and G_2-phase checkpoints after ionizing irradiation. Mol Cell Biol 2001;21:3445–50.
44. Xu B, Kim ST, Lim DS, Kastan MB. Two molecularly distinct G_2/M checkpoints are induced by ionizing irradiation. Mol Cell Biol 2002;22:1049–59.
45. Yarden RI, Pardo-Reoyo S, Sgagias M, Cowan KH, Brody LC. BRCA1 regulates the G_2/M checkpoint by activating Chk1 kinase upon DNA damage. Nat Genet 2002;30:285–9.

BRCA1 Promotes Induction of ssDNA by Ionizing Radiation

Brian P. Schlegel, Francine M. Jodelka and Rafael Nunez

Cancer Res 2006;66:5181-5189.